Stability of Neuronal Networks with Homeostatic Regulation

Daniel Harnack, Miha Pelko, Antoine Chaillet, Yacine Chitour, Mark Van Rossum

Stability of neuronal networks with homeostatic regulation

Daniel Harnack[1+*], Miha Pelko[1*], Antoine Chaillet[2], Yacine Chitour[2], Mark C.W. van Rossum[1†]

September 23, 2014

[1]School of Informatics, Informatics Forum, 10 Crichton Street, Edinburgh, EH8 9AB, UK
[2]L2S - Univ. Paris Sud 11 - Supélec, 3, rue Joliot-Curie, 91192 Gif-sur-Yvette, France
[+]Current address: Institute of Theoretical Physics, University of Bremen, Bremen, Germany
[*] These authors contributed equally.
[†]Corresponding author: mvanross@inf.ed.ac.uk

Abstract

Neurons are equipped with homeostatic mechanisms that counteract long-term perturbations of their average activity and thereby keep neurons in a healthy and information-rich operating regime. Yet, systematic analysis of homeostatic control has been lacking. The analysis presented here reveals two important aspects of homeostatic control. First, we consider networks of neurons with homeostasis and show that homeostatic control that is stable for single neurons, can destabilize activity in otherwise stable recurrent networks leading to strong non-abating oscillations in the activity. This instability can be prevented by dramatically slowing down the homeostatic control. Next, we consider the case that homeostatic feedback is mediated via a cascade of multiple intermediate stages. Counter-intuitively, the addition of extra stages in the homeostatic control loop further destabilizes activity in single neurons and networks. Our theoretical framework for homeostasis thus reveals previously unconsidered constraints on homeostasis in biological networks, and provides a possible explanation for the slow time-constants of homeostatic regulation observed experimentally.

Author summary

Despite their apparent robustness many biological system work best in controlled environments, the tightly regulated mammalian body temperature being a good example. Homeostatic control systems, not unlike those used in engineering, ensure that the right operating

conditions are met. Similarly, neurons appear to adjust the amount of activity they produce to be neither too high nor too low by, among other ways, regulating their excitability. However, for no apparent reason the neural homeostatic processes are very slow, taking hours or even days to regulate the neuron. Here we use methods from mathematical control theory to show that if this weren't the case, in particular in networks of neurons the control system might otherwise become unstable and wild oscillations in the activity result. Our results lead to a deeper understanding of neural homeostasis and can help the design of artificial neural systems.

Introduction

Neurons in the brain are subject to varying conditions. Developmental processes, synaptic plasticity, changes in the sensory signals, and tissue damage can all lead to over- or understimulation of neurons. Both cases are undesirable: Prolonged periods of excessive activity are potentially damaging and energy inefficient, while prolonged low activity is information poor. Neural homeostasis is believed to prevent these situations by adjusting the neural parameters and keeping neurons in an optimal operating regime. Such a regime can be defined from information processing requirements (Laughlin, 1981; Stemmler and Koch, 1999), possibly supplemented with constraints on energy consumption (Perrinet, 2010). As homeostasis can greatly enhance computational power (Triesch, 2007; Lazar, Pipa, and Triesch, 2009; Naudé et al., 2013), and a number of diseases has been linked to deficits in homeostasis (Horn, Levy, and Ruppin, 1996; Fröhlich, Bazhenov, and Sejnowski, 2008; Chakroborty et al., 2009; Soden and Chen, 2010), it is important to know the fundamental properties of homeostatic regulation, its failure modes, and its constraints.

One distinguishes two homeostatic mechanisms: synaptic and intrinsic excitability homeostasis (Davis, 2006; Turrigiano, 2011). In case of over-excitement, synaptic homeostasis scales excitatory synapses down and inhibitory synapses up, while intrinsic homeostasis increases the firing threshold of neurons. The latter is the subject of this study. Intrinsic homeostasis correlates biophysically to changes in the density of voltage gated ion channels, (e.g. Desai, Rutherford, and Turrigiano, 1999; van Welie, van Hooft, and Wadman, 2004; O'Leary, van Rossum, and Wyllie, 2010), as well as the ion channel location in the axon hillock (Kuba, Oichi, and Ohmori, 2010; Grubb and Burrone, 2010).

All homeostatic mechanisms include an activity sensor and a negative feedback that counters deviations of the activity from a desired value. Control theory describes the properties of feedback controllers and the role of its parameters (O'Leary and Wyllie, 2011). In engineering one typically strives to bring a system rapidly to its desired state with minimal residual error.

It is reasonable to assume that neural homeostasis has to be fairly rapid too in order to be effective, although it should not interfere with the typical timescales of perceptual input or of neural processing (millisecond to seconds). However, intrinsic excitability homeostasis is typically much slower, on the order of many hours to days (Desai, Rutherford, and Turrigiano 1999; Karmarkar and Buonomano 2006; O'Leary, van Rossum, and Wyllie 2010; Gal et al. 2010, but see van Welie, van Hooft, and Wadman 2004). One hypothesis is that this is sufficiently fast to keep up with typical natural perturbations, but an alternative hypothesis, explored here, is that stable control necessitates such slow homeostasis. Note, that the speed of homeostasis is the time it takes to reach a new equilibrium after a perturbation. This does not rule out that homeostatic compensation can start immediately without delay after the perturbation; it just takes a long time to reach its final value.

In computational studies homeostatic parameters are usually adjusted by hand to prevent instability, but a systematic treatment, in particular in networks, is lacking (an exception is a recent study by Remme and Wadman (2012), see Discussion). Furthermore, homeostasis is often modeled as a simple, minimal feedback system, assuming that the details of the control loop are unimportant. Here we analyze two issues: First, we examined the stability conditions for networks of neurons equipped with homeostasis. We show that homeostasis can destabilize otherwise stable networks and that, depending on the amount of recurrence, stable homeostatic feedback needs to be much slower for networks than required for single neurons. Secondly, we asked what happens if feedback occurs via a number of intermediate stages, as is common in biological signaling cascades. We show that having additional elements in the feedback loop tends to destabilize control even further, despite the feedback being slower. The results put constraints on the design and interpretation of homeostatic control and help to understand biological homeostasis.

Results

Homeostatic framework

We first analyze a single neuron with homeostasis, a schematic is shown in Fig.1A. We describe the activity of the neuron as a function of time with a firing rate $r_1(t)$. A common approximation for the firing rate dynamics is

$$\tau_1 \frac{dr_1(t)}{dt} = -r_1(t) + g(u(t) - \theta(t)) \tag{1}$$

which can be understood as follows: The time-constant τ_1 determines how rapidly the firing rate changes in response to changes in the input and how rapidly it decays in the absence of input. We use τ_1 =10 ms. The value of τ_1 serves as the time-constant with respect to which all the other time-constants in the system will be defined. As only the ratios between time-constants will matter, the results are straightforwardly adapted to other values of τ_1.

The f-I curve $g()$ describes the relation between net input to the neuron and its firing rate. In general the f-I curve will be non-linear, but for the initial mathematical analysis we assume a linear rectifying f-I curve, $g(x) = \alpha x$ if $x > 0$ and $g(x) = 0$ otherwise. When considering the stability to small perturbations around the homeostatic set-point (local stability), a linear approximation of the f-I curve can be made. An extension to general non-linear f-I curves is presented below. We assume that homeostasis acts as a bias current which shifts the f-I curve, consistent with experimental data (e.g. O'Leary, van Rossum, and Wyllie, 2010). The total input is thus $u(t) - \theta(t)$, where $u(t)$ is proportional to external input current to the neuron, typically from synaptic input. Crucially, $\theta(t)$ is the homeostatically controlled firing threshold of the neuron. While physiologically both the threshold current and threshold voltage of neurons are affected by homeostasis (Desai, Rutherford, and Turrigiano, 1999), our model comprises both indistinguishably.

Rather than reading out the activity directly, the homeostatic controller takes its input from averaged activity. To obtain the averaged activity $r_2(t)$ of the neuron, the firing rate $r_1(t)$ is filtered with a linear first order filter with a time-constant τ_2

$$\tau_2 \frac{dr_2(t)}{dt} = -r_2(t) + r_1(t) \tag{2}$$

Biophysically, the intra-cellular calcium concentration is a very likely candidate for this sensor (Davis, 2006) in which case τ_2 is around 50ms.

The last step in the model is to integrate the difference between the average activity and the pre-defined desired activity level r_{goal}

$$\tau_3 \frac{dr_3(t)}{dt} = r_2(t) - r_{goal} \tag{3}$$

r_{goal} was set in the figures to 1Hz, but its value is inconsequential. The feedback loop is closed by setting the threshold in Eq.1 equal to this signal, that is $\theta(t) = r_3(t)$. Thus, if the activity remains high for too long, r_2 and r_3 increase, increasing the threshold and lowering the firing rate, and vice versa if the activity is below the set-point r_{goal} for too long.

Note that in contrast to the earlier equations, Eq.(3) does not have a decay term on the right hand side, i.e. a term of the form $-r_3(t)$. This means that instead of a leaky integrator, it is a perfect integrator which keeps accumulating the error in the rate $(r_2(t)-r_{goal})$ without any decay. Mathematically, this can be seen by re-writing Eq.(3) as $r_3(t) = \frac{1}{\tau_3}\int_{-\infty}^{t}[r_2(t')-r_{goal}]\,dt'$. Perfect integrators are commonly used in engineering solutions such as PID controllers and are very robust. A perfect integrator ensures that, provided the system is stable, the goal value r_{goal} is eventually always reached, as otherwise $r_3(t)$ keeps accumulating. It is straightforward to extend our theory to a leaky integrator; for small leaks, this does not affect our results. Although it might appear challenging to build perfect integrators in biology, evidence for them has been found in bacterial chemo-taxis (Saunders, Koeslag, and Wessels, 1998; Yi et al., 2000). The time-constant τ_3 is therefore not strictly a filter time-constant, but it determines how rapidly errors are integrated and thus how quickly homeostasis acts. In the limit that $\tau_3 \gg \tau_1, \tau_2$ the firing rate settles exponentially with a time-constant τ_3/α in response to a perturbation, that is, $r_1(t) - r_{goal} \propto \mathrm{e}^{-\alpha t/\tau_3}$. For arbitrary time-constants τ_1, τ_2, τ_3 the homeostatic response will generally be a mix of three exponentials. The resulting model is a 3-dimensional linear differential equation with $r_1(t)$, $r_2(t)$ and $r_3(t)$ as dependent variables.

In the linear case the gain α can be fully absorbed in τ_3. A shallower f-I curve ($\alpha < 1$) implies a weaker feedback, and is equivalent to a proportionally slower τ_3; in both cases it takes longer for the system to attain the goal value. For simplicity we set α to one without loss of generality. Note, that this manipulation will affect the input gain, but this is of no consequence in the analysis. Also note, that the compensation starts as soon as the rate diverges from the goal value, although the change in θ is initially very small.

An attentive reader might have noticed that θ is a current, while r_3 is a rate. Formally this inconsistency can be resolved by defining $\theta(t) = \beta r_3(t)$ where β has dimensions A/Hz and give α dimensions Hz/A. However, for simplicity we use dimensionless units; this does in no way affect our results. Also note, that while r_1 is assumed positive, r_3 and θ are not as they are the difference between actual and goal rate and thus can take negative values.

Stability of homeostatic control in the single neuron

While the above system is a set of piecewise linear equations, in the limit of small perturbations, that is staying away from the rectification threshold,the system of differential equations is linear. This means we can borrow results from linear control theory to examine the stability of the set of differential equations that define the neural and homeostatic dynamics. One needs to solve the differential equations and check whether the solutions diverge. Various equivalent approaches have been developed to determine stability of controllers (e.g. DiStefano, Stubberud, and Williams, 1997). Here we write the set of first order equations, Eqs.(1)-(3) in matrix form

$$\frac{d}{dt}\begin{pmatrix} r_1(t) \\ r_2(t) \\ r_3(t) \end{pmatrix} = M \begin{pmatrix} r_1(t) \\ r_2(t) \\ r_3(t) \end{pmatrix} + \mathbf{b}$$

with matrix

$$M = \begin{pmatrix} -\frac{1}{\tau_1} & 0 & -\frac{1}{\tau_1} \\ \frac{1}{\tau_2} & -\frac{1}{\tau_2} & 0 \\ 0 & \frac{1}{\tau_3} & 0 \end{pmatrix}$$

and vector

$$\mathbf{b}(t) = \begin{pmatrix} \frac{1}{\tau_1}u(t) \\ 0 \\ -\frac{1}{\tau_3}r_{goal} \end{pmatrix}$$

The theory of differential equations states that the solution to this set of equations is the sum of a particular solution (which is unimportant for our purposes) and solutions to the homogeneous equation, which is the equation with $\mathbf{b} = \mathbf{0}$. With the 'ansatz' $r_i(t) = c_i e^{\lambda t}$, one finds that in order to solve the homogeneous equation, the vector $\mathbf{c} = (c_1, c_2, c_3)$ must be an eigenvector of M with eigenvalue λ. This means that λ has to solve the characteristic polynomial, $\det(M - \lambda I) = -(1 + \tau_1\lambda)(1 + \tau_2\lambda)\tau_3\lambda - 1 = 0$. The three eigenvalues of M are in general complex numbers. The eigenvalue determines the stability of each mode as follows:

- If an eigenvalue is real and negative, the corresponding mode is stable as the exponential $\mathrm{e}^{\lambda t}$ decays to zero over time.
- If an eigenvalue is complex and the real part is negative, the corresponding mode decays over time as a damped oscillation. In the context of homeostasis such activity oscillations might be biologically undesirable, in particular when they persist for many cycles.

- Finally, the solution will diverge if any of the eigenvalues has a positive real part. In practice, some mechanism, such as a squashing or rectifying f-I curve, will restrain the firing rate and strong non-abating oscillations in the firing rate will occur. (for two dimensional systems this can be proven using the Poincare-Bendixson theorem e.g. Khalil, 2002).In this case homeostatic control is called unstable.

Which of these above scenarios occurs depends in our model solely on the ratio between the three τ_i parameters. In most of what follows, we determine the required value of τ_3 for given τ_1 and τ_2.

Fig. 1B shows simulated responses of the firing rate $r_1(t)$, and the threshold variable $r_3(t)$ to a step input for various settings of the time-constants. It can be observed that only for extremely short values of τ_3 the neuron is unstable (striped region). In this case the firing rate oscillates continuously and information coding is virtually impossible. In the gray region the neuron is stable but displays damped oscillations after changes in the activity. Stability without oscillation (white region) can always be achieved by taking τ_3 slow enough. The explicit stability condition follows from the Routh–Hurwitz stability criterion and is $\tau_3 > \tau_1\tau_2/(\tau_1 + \tau_2)$ (see Methods).

Our main assumption is that instability is to be avoided at all cost. While oscillations by themselves occur in many circumstances in neuroscience and can have functional roles, the oscillations here are uncontrollable and can not be stopped. The oscillating state is almost the opposite of homeostasis, as neurons would only be able to code very little information. Finally, the oscillating state is metabolically costly, especially if excitability is regulated through the insertion and removal of ion-channels.

The above results confirm the intuition that slower feedback is more stable than fast feedback. When τ_2 is 50ms, τ_3 needs to be longer than 8ms to obtain stability. To warrant the absence of damped oscillations a similar criterion can be derived (Methods, Eq. 12) and in this example case τ_3 needs to be longer than 220ms to avoid oscillations. In summary, for single neurons simple homeostatic control is stable even when it is very fast. Therefore, the stability of the homeostatic controller would not appear an issue for homeostasis of intrinsic excitability. Such very fast homeostasis might not even be desirable, because it will filter out components of the input that are slower than the homeostatic control. For instance in Fig. 1B (top left), the neural response equals the stimulus with changes slower than $\sim$100ms filtered out.

Finally note, that because the system is linear, the instability will be triggered by any size or type of perturbation, whether transient or sustained.

Stability in recurrent networks

Next, we consider a network of N neurons and again analyze the stability of homeostatic control. The network is connected with fast synapses via an $N \times N$ weight matrix W. For ease of presentation we assume W to be symmetric, but this condition can be relaxed at the cost of more complicated stability conditions (see Methods). In this abstract network a synapse can be excitatory or inhibitory; imposing Dale's principle will affect the eigenvalue spectrum of the weight matrix (Rajan and Abbott, 2006), but does not alter our result otherwise.

For networks the conditions on homeostatic control are much more stringent than for single neurons. In Fig.2A the population firing rate of a simulated network is plotted as the recurrence is increased while all other network and homeostasis parameters are kept the same (left to right plot). Increasing the recurrence in the network leads to strong, persistent oscillations. Importantly, without homeostasis the network is stable (top panels, dotted curves). To prevent instability the feedback needs to be much slower in networks than for single neurons.

This required slowdown of homeostatic control can be understood as follows: In the absence of homeostasis the firing rate dynamics obeys

$$\tau_1 \frac{d}{dt}\mathbf{r}_1(t) = (W - I)\mathbf{r}_1(t) + \mathbf{u}(t)$$

where $\mathbf{r}_1(t)$ is a N-dimensional vector containing all firing rates in the network, and $\mathbf{u}(t)$ is a vector of external input to the neurons in the network. The recurrent feedback is contained in the term $W\mathbf{r}_1(t)$. These types of symmetric networks have been used in many applications, such as noise filtering and evidence accumulation (Dayan and Abbott, 2002). We denote the eigenvalues of W with w_n. We definethe largest eigenvalue, $w_m = \max(w_n)$, as the *recurrence* of the network. The recurrent excitatory connectivity slows down the effective time-constant of a given mode (Dayan and Abbott, 2002; van Rossum et al., 2008). This can be seen by writing the equation for each mode as $\frac{\tau_1}{1-w_n}\frac{dr_n(t)}{dt} = -r_n(t) + \frac{1}{1-w_n}u_n(t)$, from which the time-constant of a given mode is then identified as $\tau_1/(1-w_n)$. The network time-constant is defined as the time-constant of the slowest mode, i.e. $\tau_1/(1-w_m)$. The network activity is stable as long as $w_m < 1$.

In the presence of homeostatic regulation, the system becomes $3N$-dimensional. It is described by the rate of each neuron $\mathbf{r}_1$, its filtered version $\mathbf{r}_2$, and its threshold $\mathbf{r}_3$. The corresponding differential equation is

$$\frac{d}{dt}\begin{pmatrix}\mathbf{r}_1\\ \mathbf{r}_2\\ \mathbf{r}_3\end{pmatrix} = M\begin{pmatrix}\mathbf{r}_1\\ \mathbf{r}_2\\ \mathbf{r}_3\end{pmatrix} + \begin{pmatrix}\frac{1}{\tau_1}\mathbf{u}(t)\\ 0\\ -\frac{1}{\tau_3}\mathbf{r}_{goal}\end{pmatrix}$$

where M is now a block-matrix, given by

$$M = \begin{pmatrix} \frac{1}{\tau_1}(W - I) & 0 & -\frac{1}{\tau_1}I \\ \frac{1}{\tau_2}I & -\frac{1}{\tau_2}I & 0 \\ 0 & \frac{1}{\tau_3}I & 0 \end{pmatrix} \tag{4}$$

We proceed as above to determine the stability of this system. In analogy with the single neuron case, there are three eigenvalues for the full system per eigenvector of W, so that we obtain $3N$ eigenvalues. In principle, one should now research the stability of each eigenvector of W. Yet the analysis can be simplified. In a network without homeostasis the most critical mode is the one with the largest eigenvalue. This also holds in networks with homeostasis: the network is stable if and only if this mode is stable (see Methods for proof). Thus, rather than analyzing the full network, we only need to analyze the stability of this most critical mode, which is given by a three dimensional system similar to the single neuron system studied above with the pre-factor of $r_1(t)$ on the right hand side as only modification,

$$\tau_1 \frac{dr_1(t)}{dt} = [w_m - 1]r_1(t) + u(t) - \theta(t) \tag{5}$$

The other equations for homeostatic control, Eqs.2 and 3, remain unchanged. The resulting three dimensional system describes the dynamics of the critical eigenmode and its homeostatic variables. The stability is now determined by the roots of the polynomial

$$(1 - w_m + \tau_1\lambda)(1 + \tau_2\lambda)\tau_3\lambda + 1 = 0 \tag{6}$$

The network is again stable if all roots have a negative real part. Application of the Routh–Hurwitz criterion (Methods) yields the stability condition $\tau_3 > \tau_3^{crit}$, where

$$\tau_3^{crit} = \frac{1}{1 - w_m} \frac{\tau_1\tau_2}{\tau_1 + (1 - w_m)\tau_2} \tag{7}$$

In Figure 2B we vary the integration time of the network by changing w_m and plot the values for τ_3 required for stability. The minimal, critical value of τ_3 is shown with the solid black curve. Eq.7 yields for $(1 - w_m)\tau_2 \gg \tau_1$ that $\tau_3 \gtrsim \tau_1/(1 - w_m)^2$, while for $(1 - w_m)\tau_2 \ll \tau_1$ this can be approximated as $\tau_3 \gtrsim \tau_2/(1 - w_m)$. When, for example, the network has an integration time-constant of 1s, τ_3 needs to be at least 4.8s to prevent instability. If the network integration time-constant is 10s, this increases to 50s.

Oscillation-free homeostasis

The sustained oscillations associated to the instability are disastrous for neural information processing as they hinder information coding, yet are energetically expensive. Damped oscillations are less harmful. However, in particular for strongly recurrent networks, damped oscillations can interfere with the desired network response. As an illustration of this we show the response of an ideal leaky integrator, such as might be used for evidence integration in Fig. 2C (gray curve). When rapid homeostasis is active, the response shows strong oscillations that occludes the network's integrative properties (black curve). Only when homeostasis is made so slow that no damped oscillations occur (dashed curve), the response approximates that of the ideal integrator.

The value of τ_3 required to ensure homeostasis without damped oscillations is much larger than the value required to prevent persistent oscillation, compare dashed curve to solid curve in Fig.2B. Interestingly, as is shown in the Methods, for long integration times it increases as the square of the integration time (slope of 2 on the log-log plot). For example if the network integration time-constant is 1s, the minimal homeostatic time-constant is 420s to prevent oscillations. And if the network integration time-constant is 10s, a realistic value in for instance working memory networks (e.g. Seung et al., 2000), this values increases to 11hrs. In summary, in particular if an oscillation-free response is required, strongly recurrent networks with long time-constants require homeostasis many orders of magnitudes slower than single neurons.

Variability and heterogeneity

To examine the generality of the results we included variability and heterogeneity in the model. First, we wondered whether heterogeneity in the time-constants, likely to occur in real neurons, could prevent the synchronous oscillations associated to the instability. Hereto we drew for each neuron the homeostatic time-constants from a gamma-distribution with an adjustable coefficient of variation (CV) and a given mean. To quantify the destabilizing effect of homeostasis, we defined the dimensionless *critical recurrence strength* w_c. It is the maximal recurrence for which the network is still stable, possibly with damped oscillations. That is, w_c is the value for which the real part of the largest eigenvalue crosses zero. For networks without homeostasis, the critical recurrence is one, but homeostasis limits this to lower values.

Stability is again determined by the stability matrix of Eq.4, however, in the heterogeneous case the dimension reduction is not possible and the spectrum of the full matrix was examined. When the CV is zero, all neurons have the same set of time-constants and the stability corresponded to that of the homogeneous networks. As the CV increased, the average maximal

allowed recurrence first increased slightly after which it decreased, Fig.3A. Moreover, as can be seen from the error bars, for a given realization of the time-constants, the stability can either be higher or lower than that of the homogeneous network. Hence random heterogeneity of the time-constants does not robustly lead to increased stability. A similar effect of heterogeneity on the transition between the damped oscillatory and oscillation-free regime is observed (not shown).

Next, we added noise to the neurons and analyzed how this affected the transition to instability. The noise might potentially have a stabilizing effect by de-synchronizing the population. Gaussian noise with a correlation time of 1ms and a standard deviation equivalent to 0.1Hz was added to the input. We measured the fluctuations as the standard deviation of the population firing rate once the system had reached steady state, Fig.3B. These fluctuations comprise both the effect of noise and the periodic oscillations caused by the instability. As seen above, Fig.2A), without noise fluctuations are absent when the recurrence is less than the critical amount, and are strong above this point, Fig.3B (dashed curve). With noise, fluctuations are always present (solid curve) and increase close to the transition to instability. Above the transition point the fluctuations are similar to the noise-free model. In a network with homeostasis the resulting fluctuations were always larger than without (grey line). The reason is that in the homeostatic network the noise is continuously exciting a damped resonant system, amplifying the fluctuations. Importantly, the amount of recurrence at which the transition to the unstable regime occurs, does not shift with noise, implying that noise does not increase stability. Rather, one can observe that in particular in the stable regime, but close to the transition to instability (around a recurrence of 0.75), homeostasis actually increases the fluctuations in the population firing rate (black curve is above gray curve) .

Spiking networks

Next, we compared the theory to simulations of networks of spiking neurons (see Methods). The connection strength was such that the network was stable and a Gaussian white noise term was injected to all neurons to prevent population synchrony. The homeostatic control was implemented exactly as above: the average rate $r_2(t)$ was extracted by filtering the spikes (τ_2 =50ms), and this was fed into the integrator as above. The homeostatic target rate was set to 4Hz.

In this asynchronous regime, the population firing rate of the spiking network can be reasonably approximated by the rate equation with a non-linear f-I curve (Eq.1) and recurrent feedback. In order to be able to compare the spiking network to the theory we turned homeostasis off and gave small step stimuli to the network and measured how quickly the firing rate equilibrated as a function of the connection strength, Fig. 4A. In the rate model this equili-

bration time is $\tau_1/(1-w_m)$. A fit to this relation gave $\tau_1 \approx (11.5 \pm 1.5)$ms and also yielded the proportionality between the synaptic strength and w_m, which we calibrated as above so that $w_m = 1$ corresponds to the critical amount of recurrence in the model without homeostasis. As the networks with close to critical recurrence are slow and difficult to simulate, we used a value of w_m=0.6, so the required homeostatic time-constants are fairly short.

According to linear stability theory analogous to Eq.7, the critical value of τ_3 is given by,

$$\tau_3^{lin} = \tilde{g}'(0)\tau_3^0 \tag{8}$$

where $\tau_3^0 = \tau_1\tau_2/[\tau_1 + (1-w_m)\tau_2]$. Furthermore, $\tilde{g}(x)$ is defined as the re-centered f-I curve such that its origin $\tilde{g}(x=0) = 0$ corresponds to the homeostatic set-point, $\tilde{g}'(0)$ is the slope of the network f-I curve at the set-point. We measured the f-I relation by turning homeostasis off and stimulating the network with increasing levels of mean current and measured the resulting mean population firing rate once the network stabilized. The linear criterion yields that when $\tau_3 \geq \tau_3^{lin}$ =64ms the network should be stable. However, the simulated network is less stable than the criterion predicts, as the network shows strong oscillations for such rapid homeostasis, Fig. 4C, second plot from below.

The reason is that the f-I curve $g()$ is non-linear. It can be shown that the system is *guaranteed* to be stable only when for all x

$$0 < \frac{\tilde{g}(x)}{x} < \frac{\tau_3}{\tau_3^0} \tag{9}$$

An f-I curve that exceeds these bounds can lead to instability given the right perturbation, despite a shallow slope at the set-point. The criterion is expressed graphically in Fig. 4B (dotted line) and corresponds to requiring that the f-I curve is enveloped by the line $y = r_{goal}$ (always satisfied here) and the line through the set-point with slope τ_3/τ_3^0. Hence the critical time-constant is $\tau_3^{aiz} = \max_x \left(\frac{\tilde{g}(x)}{x}\right)\tau_3^0$. The criterion is known as the Aizerman conjecture (e.g. Leigh, 2004), and although not generally true, it is known to hold for this particular 3 dimensional system (Fujii and Shoji, 1972). Note that for a linear system $\tilde{g}(x)/x$ is constant and one retrieves Eq. 8.

When applied to our simulations the criterion leads to a value of $\tau_3^{aiz} = 322$ms. This indeed leads to stable homeostasis, Fig. 4C, top. In simulations a minimal value of τ_3 around $\tau_3 = 240$ms was already enough to stabilize the network. This is not in conflict with the theory: not satisfying the criterion does not necessarily lead to instability, in other words Eq.9 is not a tight bound.

Cascaded homeostatic control

The above results assumed a simple controller with only three components in the feedback loop, r_1, r_2, and r_3, but homeostatic control of excitability has many intermediate stages, for instance synthesis, transport and insertion of ion-channels is likely involved. Therefore we asked how the stability of homeostatic control changes with longer feedback cascades. Our intuition was that adding more elements to the feedback cascade slows down the feedback, and therefore would increase stability. However, we found that adding more filters actually de-stabilizes the network.

We first simplify our model from three to two filters, and analyze what happens to the critical amount of network recurrence if we add a third filter, Fig.5A. With two filters ($\tau_1 = 10ms$, $\tau_2 = 50ms$) the critical recurrence is one, the same as for a network without homeostasis (gray curve). The addition of a third filter, such that the time-constants are $(\tau_1, \tau_2, \tau_3) = (10, 50, \tau)$ is destabilizing even if the third filter has a time-constant slower than any other time-constant (dashed curve). Only for a very long time-constant it had no detrimental effect. Alternatively, one can add an intermediate filter, such that the time-constants are $(\tau_1, \tau_2, \tau_3) = (10, \tau, 50)$. Also this is destabilizing (solid line). In this case the destabilizing effect can be minimized by taking τ as short as possible. The filter then has a negligible effect, and the system resembles the two filter system again.

More generally, assuming that there is no intermediate feedback between the filters and that each element can be approximated by a linear filter, our formalism can be extended to an arbitrary number of intermediate elements in the feedback loop. Suppose that we have K filters, each with its own time-constant τ_k. The threshold is taken from the K-th filter, i.e. $\theta(t) = r_K(t)$. We thus have

$$\begin{aligned}
\tau_1 \frac{dr_1(t)}{dt} &= -[1 - w_m] r_1(t) + u(t) - r_K(t) \\
\tau_k \frac{dr_k(t)}{dt} &= -r_k(t) + r_{k-1}(t) \qquad k = 2 \ldots K-1 \\
\tau_K \frac{dr_K(t)}{dt} &= -r_{goal} + r_{K-1}(t)
\end{aligned}$$

The corresponding characteristic polynomial in this case is

$$1 + \lambda\tau_K(1 - w_m + \lambda\tau_1) \prod_{k=2}^{K-1} (1 + \lambda\tau_k) = 0 \tag{10}$$

This expression is invariant to permutations of the time-constants $\tau_2, \ldots, \tau_{K-1}$. The stability is again determined by the real part of the solutions to the polynomial. As analytic results

such as Routh-Hurwitz analysis, quickly grow in complexity for an increasing number of filters, we solve polynomial Eq.10 numerically.

As the time-constants or even the number of steps in the homeostatic feedback in neurons is not known, we examined the stability with various hypothetical settings of the additional filters, Fig.5B. When the time-constants were set linearly increasing as $\tau_i = 10, 100, 200, 300, \ldots$.ms, the stability decreased most strongly as the number of stages K increased (dashed curve). Using $\tau_i = 10, 500, 500, \ldots, 500, 5000$, stability decreased also with the number of filters (dot-dashed curve). When the time-constants were set exponentially as $\tau_i = 10, 20, 40, 80 \ldots$ stability decreased when using only few filters, and leveled off with more filters (black curve). With a stronger exponential increase $\tau_i = 10, 30, 90, 270 \ldots$ the stability reached a minimum for 4 filters and then increased to a constant level (thick black curve). Thus in general addition of filters does not lead to stabilization of the system.

Next we wondered what choice of time-constants will be most stable for a given number of filters. Suppose a cascade where the time-constant of the firing rate τ_1 and of the threshold setting τ_K are fixed. In analogy with the three filter network, setting the time-constants of the intermediate stages as short as possible is the most stable configuration. Even adding an intermediate filter with a time-constant much slower than τ_K will not stabilize the system. The intuition behind these results is that not only the speed of the feedback matters, but its phase delay matters as well. With sufficient filtering the negative homeostatic feedback will be out of phase with the firing rate, amplifying perturbations. This effect is similar to the typically destabilizing effect of delays in control theory.

The interaction between network recurrence and the presence of multiple feedback filters can be analyzed with Eq.10 as well. As an example, consider the case where τ_1=10ms, τ_2 = 20ms, and $w_m = 0.99$. If w_m increases to 0.995 the required τ_3 doubles from 4.7 to 9.7 s. Alternatively, adding an intermediate filter with a time-constant of 50ms also approximately doubles the required time-constant of the integrator to 9.5s. Now increasing both w_m and increasing the number of filters quadruples the required τ_3 to 19.5s, thus the effect of recurrence and cascade length are complementary.

Discussion

We have, to our knowledge for the first time, systematically analyzed instabilities in the neural activity that arise from homeostasis of intrinsic excitability. In the worst case, homeostasis can lead to continuous oscillations of the activity. Homeostasis can also give rise to damped oscillations, which are less disastrous to information processing, provided the oscillations don't persist too long. To our knowledge such damped oscillations in the homeostatic response

have not been observed experimentally, although averaging of experimental data could have obscured their detection. Nevertheless, we think that they are unlikely to occur in biology because substantial cost is involved in alternating up-down regulation of excitability, and because the homeostatic control can strongly interact with the network activity (Fig. 2C).

Our control theoretic framework for homeostasis sets precise constraints on homeostatic control to prevent either form of instability. We find that a typical single neuron model with just a few filters in the feedback loop has no stability issues even when the homeostatic control is very fast. However, this is no longer true when network interactions are included. The stronger the recurrence of the network, the slower the feedback needs to be. Networks with time-constants on the order of seconds have been proposed to explain sensory evidence integration, decision making and motor control (Seung et al., 2000; Gold and Shadlen, 2007; Goldman and Wang, 2009). The minimal homeostatic for homeostasis to be oscillation-free scales quadratically with the network time-constant. As a result the required homeostasis can easily be on the order of hours, a value comparable to experimentally observed homeostatic action (Desai, Rutherford, and Turrigiano, 1999; Karmarkar and Buonomano, 2006; O'Leary, van Rossum, and Wyllie, 2010; Gal et al., 2010).

Stability typically decreases further when the number of stages in the feedback loop increases, Fig. 5. This effect complements the effect of the recurrence, so that for recurrent networks consisting of neurons with long homeostatic cascades, even slower homeostasis is required. The instability can not be prevented by including heterogeneity or adding noise to the system and is also found in spiking network simulations.

Most of our analysis was based on a linearization of the dynamics of the neuron and the feedback loop. This is appropriate to calculate the homeostatic response to small perturbations. Obviously stability to small perturbations is needed when stability to arbitrary size perturbations is required. In addition, we have derived the condition for stability if the f-I curve is non-linear to arbitrary size perturbations and found that a non-linear f-I curve further limits the minimal homeostatic time-constant. Ideally, one would like to know the stability requirements for any given non-linear homeostatic controller. However, only in a very limited number of cases extensions of our mathematical results to either multiple non-linearities in the control loop or to higher dimensional systems (i.e. with longer feedback cascades) are known.

It is not unreasonable to assume that biology uses multiple, parallel homeostatic regulators. Some cases can be captured by our theory, for instance if multiple feed-backs use the same error signal, stability is determined by the quickest feedback, so that our results are easily adapted to that case. However, a general theory of such systems is lacking. It would be very interesting to know whether biology uses parallel regulators to increase stability.

Stability of homeostatic control has been the main consideration in this study. This is of

course of utmost importance biologically, but it is unlikely to be the only criterion. There can also be cases where rapid acting homeostasis is needed. For instance, one might want to minimize periods of prolonged hyperactivity, while in a recent study fast *synaptic* homeostasis was required to counter synaptic plasticity (Zenke, Hennequin, and Gerstner, 2013). It suggests that homeostatic control is constrained "from below and from above", and therefor more finely tuned than previously thought. Unfortunately data on the time-course of the homeostasis of intrinsic excitability, its mediators and regulation cascade is limited, hindering a direct comparison of data to our analysis. Nevertheless, a number of predictions follows from this work: we predict homeostasis to be slower in brain regions with strong recurrent connections and long network integration times. Secondly, we predict that intermediate steps in the homeostatic feedback cascade are rapid so as to prevent instability.

We note that the introduced framework is very general. A recent study examined simple homeostatic control for a network with separate excitatory and inhibitory populations and found that excitatory neurons require faster homeostasis than inhibitory neurons (Remme and Wadman, 2012). Our results can be used to extend those results to more realistic control loops. Other targets for extension and application of this theory include excitatory/inhibitory balanced networks, controllers with parallel slow and fast components, as well as models that include dynamical synapses. Also the interaction with 'Hebbian' modification of the intrinsic excibility (Janowitz and van Rossum, 2006) will be of interest. Finally, these results might be important for other regulatory feedback systems such as synaptic homeostasis and spike frequency adaptation.

Acknowledgments

We would like to thank Matthias Hennig and Tim O'Leary for discussions.

Methods

Stability in recurrent network

In the main text we state that stability of a homeostatic network is determined by the stability of the mode with the largest eigenvalue. Here we prove that if the reduced model is stable, then so is the full network model. Given the interaction matrix M of the full network, Eq. 4, it is easy to show that eigenvectors of the matrix M have the form $\begin{pmatrix} \mathbf{e}_n \\ \alpha_n \mathbf{e}_n \\ \beta_n \mathbf{e}_n \end{pmatrix}$, where $\mathbf{e}_n$ is a eigenvector of the W matrix, and α_n and β_n are complex numbers. This means that the filtered firing rates (the vectors $\mathbf{r}_2$ and $\mathbf{r}_3$) follow the firing rates $\mathbf{r}_1$ with a phase lag and arbitrary amplitude. We use that the symmetric $N \times N$ matrix W is diagonizable by an orthogonal matrix, that is $W = U^T D U$, where D is a diagonal matrix with the eigenvalues w_n on the diagonal and $UU^T = I$. We analyze M in the eigenspace of W using the matrix $U_{3N} = U \otimes I_3$, where $\otimes$ is the Kronecker product. In these coordinates $\overline{M} = U_{3N} M U_{3N}^T$ and equals

$$\overline{M} \;=\; \begin{pmatrix} \frac{1}{\tau_1}(D-I) & 0 & -\frac{1}{\tau_1} I \\ \frac{1}{\tau_2} I & -\frac{1}{\tau_2} I & 0 \\ 0 & \frac{1}{\tau_3} I & 0 \end{pmatrix}$$

In these coordinates, there is no interaction between the various eigenmodes. The stability of each mode is given by Eq. 7. Because the factor $(1-w_n)$ is positive and minimal for $w_n = w_m$, stability of the eigenmode with eigenvalue w_m implies stability for all other modes for which $w_n \leq w_m$.

The stability condition is found from the Routh–Hurwitz stability criterion (DiStefano, Stubberud, and Williams, 1997). It states that the third order polynomial $\sum_{i=0}^{3} c_i \lambda^i = 0$ has exclusively negative roots when 1) all the coefficients c_i are larger than zero, and 2) $c_0 c_3 < c_1 c_2$. Applied to homeostatic control this yields Eq.7.

Non-symmetric networks

The analysis can be extended to networks with non-symmetric weight matrices. Symmetry of W implies that the eigenvalues of the matrix W are real. For non-symmetric W, the eigenvalues are no longer guaranteed to be real but can be complex. The Routh-Hurwitz criterion needs now to be applied after splitting the real and imaginary part of the polynomial. The conditions that guarantee negative real parts for the solutions of the polynomial $\lambda^3 + c_1\lambda^2 + c_2\lambda + c_3 =$

0 with complex coefficients c_i are (Zahreddine and Elshehawey, 1988): 1) $\Re(c_1) > 0$, 2) $\Re(c_1)\Re(c_1\bar{c}_2 - c_3) - \Im(c_2)^2 > 0$, and 3) $[\Re(c_1)\Re(c_1\bar{c}_3) - \Re(c_3)^2][\Re(c_1)\Re(c_1\bar{c}_2 - c_3) - \Im(c_2)^2] - [\Re(c_1)\Im(\bar{c}_1 c_3) - \Re(c_3)\Im(c_2)]^2 > 0$, where $\bar{c}$ denotes the complex conjugate, and $\Re$ and $\Im$ the real and imaginary parts. In this case one has $c_1 = 1/\tau_2 + (1 - w_n)/\tau_1$, $c_2 = (1 - w_n)/\tau_1\tau_2$, $c_3 = 1/\tau_1\tau_2\tau_3$, where w_n is the complex eigenvalue. Splitting the real and imaginary part as $w_n = w_r + iw_i$, these conditions combine to the condition $\tau_3 \geq \tau_3^{cc}$ with

$$\tau_3^{cc} = \frac{1}{1 - w_r} \frac{\tau_1\tau_2[\tau_1 + (1 - w_r)\tau_2] + \frac{1}{2}\tau_2^3 w_i^2[1 + \sqrt{1 + 4\tau_1(1 - w_r)/(\tau_2 w_i^2)}]}{[\tau_1 + (1 - w_r)\tau_2]^2 + w_i^2\tau_2^2} \tag{11}$$

In contrast to the case of symmetric W, these conditions have to be checked for all N eigenvalues of W. In the case of random, excitation-only networks the largest eigenvalue is typically real, so the theory of the main text can be applied. Furthermore, by taking the limit of infinite w_i it can be shown that stability is guaranteed for any complex w_n when $\tau_3 > \tau_2/(1 - w_r)$, which is more stringent than the condition given in Eq.7. Under this condition any network, including non-symmetric ones, is guaranteed to be stable.

Oscillation-free response

To guarantee an oscillation-free response of the network, the eigenvalues need to be negative and real. For a given w_n this means that all the solutions of the polynomial

$$P(\lambda) = (1 - w_n + \tau_1\lambda)(1 + \tau_2\lambda)\tau_3\lambda + 1$$

have to be real. As in our analysis above, the largest eigenvalue of W is the most critical one so that we only need to study the case $w_n = w_m$.

The polynomial is a cubic; it is negative for negative λ and positive for positive λ. For all solutions to be real, the polynomial has to dip down after the first zero-crossing and cross zero again, after which it crosses the x-axis a final time. The condition on the minimum of the dip, given by $P'(\lambda_c) = 0$ and $P''(\lambda_c) > 0$, is that it should be below zero, i.e. $P(\lambda_c) < 0$. This yields the condition $\tau_3 \geq \tau_3^{co}$ with

$$\tau_3^{co} = \frac{1}{(1 - w_m)^2(\tau_1 - \tau_2')^2}\left[(\tau_1 - 2\tau_2')(2\tau_1 - \tau_2')(\tau_1 + \tau_2') + 2(\tau_1^2 - \tau_1\tau_2 + \tau_2^2)^{3/2}\right] \tag{12}$$

where we defined $\tau_2' = (1 - w_m)\tau_2$. In the limit of strong recurrence $\tau_3^{co} = \frac{4}{\tau_1}\left(\frac{\tau_1}{1 - w_m}\right)^2$, which implies that the required time-constant τ_3 scales quadratically with the network time-constant, $\tau_1/1 - w_m$.

Spiking network simulations

A population of 16000 linear integrate-and-fire neurons was coupled with a 2% connection probability via excitatory synapses modeled as exponentially decaying conductances (5ms synaptic time-constant). It is possible to add inhibitory connections to the network, but as long as the network remains in the mean-driven regime this should not affect the results. The membrane voltage of each neuron obeyed $\tau_{mem}\frac{dV(t)}{dt} = -V(t) + V_{rest} + RI(t)$, where $t_{mem} =$ 20ms, V_{rest}= -60mV and $R = 1\text{M}\Omega$. In addition, upon reaching the threshold (V_{thr}=-50mV) the voltage reset ($V_{reset} = V_{rest}$, 5ms refractory period). The current I consisted of recurrent input, external drive and homeostatic bias, $I(t) = g_e(t)(V(t) - E_e) + I(t) - hr_3(t)$. The factor h converts the filtered firing rate r_3 to a current and sets the strength of the homeostatic control. It was set to $1pA/Hz$. The homeostatic control was implemented as in the rate based networks: the average rate $r_2(t)$ was extracted by filtering the spikes (τ_2 =50ms), and this was fed into the integrator. The homeostatic target rate was set to 4Hz. The external current $I(t)$ contains both stimulation and a Gaussian white noise term ($\sigma = 75\text{pA}$) to prevent population synchrony.

References

Chakroborty, S., I. Goussakov, M. B. Miller, and G. E. Stutzmann (2009). Deviant ryanodine receptor-mediated calcium release resets synaptic homeostasis in presymptomatic 3xTg-AD mice. *J Neurosci* 29(30): 9458–9470.

Davis, G. W. (2006). Homeostatic control of neural activity: from phenomenology to molecular design. *Annu Rev Neurosci* 29: 307–323.

Dayan, P. and L. F. Abbott (2002). *Theoretical Neuroscience*. MIT press, Cambridge, MA.

Desai, N. S., L. C. Rutherford, and G. G. Turrigiano (1999). Plasticity in the intrinsic electrical properties of cortical pyramidal neurons. *Nat. Neuro.* 2: 515–520.

DiStefano, J. J., A. J. Stubberud, and I. J. Williams (1997). *Schaum's Outline of Feedback and control Systems*. McGraw-Hill Professional.

Fröhlich, F., M. Bazhenov, and T. J. Sejnowski (2008). Pathological effect of homeostatic synaptic scaling on network dynamics in diseases of the cortex. *J Neurosci* 28(7): 1709–1720.

Fujii, K. and K. Shoji (1972). Verification of the Aizerman and/or Kalman conjecture. *Automatic Control, IEEE Transactions on* 17(3): 406–408.

Gal, A., D. Eytan, A. Wallach, M. Sandler, J. Schiller, and S. Marom (2010). Dynamics of excitability over extended timescales in cultured cortical neurons. *J Neurosci* 30(48): 16332–16342.

Gold, J. I. and M. N. Shadlen (2007). The neural basis of decision making. *Annu Rev Neurosci* 30: 535–574.

Goldman, M.S., C. A. and X. Wang (2009). Neural integrator models. In Squire, L., editor, *Encyclopedia of Neuroscience*, pp. 165–178. Oxford: Academic Press.

Grubb, M. S. and J. Burrone (2010). Activity-dependent relocation of the axon initial segment fine-tunes neuronal excitability. *Nature* 465(7301): 1070–1074.

Horn, D., N. Levy, and E. Ruppin (1996). Neuronal-based synaptic compensation: a computational study in Alzheimer's disease. *Neural Comput* 8(6): 1227–1243.

Janowitz, M. K. and M. C. W. Rossum (2006). Excitability changes that complement Hebbian learning. *Network* 17: 31–41. submitted.

Karmarkar, U. R. and D. V. Buonomano (2006). Different forms of homeostatic plasticity are engaged with distinct temporal profiles. *Eur J Neurosci* 23(6): 1575–1584.

Khalil, H. K. (2002). *Nonlinear systems*. Prentice hall Upper Saddle River, 3 edition.

Kuba, H., Y. Oichi, and H. Ohmori (2010). Presynaptic activity regulates Na^+ channel distribution at the axon initial segment. *Nature* 465(7301): 1075–1078.

Laughlin, S. B. (1981). A simple coding procedure enhances a neuron's information capacity. *Zeitschrift für Naturforschung* 36: 910–912.

Lazar, A., G. Pipa, and J. Triesch (2009). SORN: a self-organizing recurrent neural network. *Front Comput Neurosci* 3: 23.

Leigh, J. J. R. (2004). *Control theory: A Guided Tour*, Vol. 64. IET.

Naudé, J., B. Cessac, H. Berry, and B. Delord (2013). Effects of cellular homeostatic intrinsic plasticity on dynamical and computational properties of biological recurrent neural networks. *J Neurosci* 33(38): 15032–15043.

O'Leary, T., M. C. W. Rossum, and D. J. A. Wyllie (2010). Homeostasis of intrinsic excitability in hippocampal neurones: dynamics and mechanism of the response to chronic depolarization. *J Physiol* 588(Pt 1): 157–170.

O'Leary, T. and D. J. A. Wyllie (2011). Neuronal homeostasis: time for a change? *J Physiol* 589(Pt 20): 4811–4826.

Perrinet, L. U. (2010). Role of homeostasis in learning sparse representations. *Neural Comput* 22(7): 1812–1836.

Rajan, K. and L. F. Abbott (2006). Eigenvalue spectra of random matrices for neural networks. *Phys Rev Lett* 97(18): 188104.

Remme, M. W. H. and W. J. Wadman (2012). Homeostatic scaling of excitability in recurrent neural networks. *PLoS Comput Biol* 8(5): e1002494.

Saunders, P. T., J. H. Koeslag, and J. A. Wessels (1998). Integral rein control in physiology. *J Theor Biol* 194(2): 163–173.

Seung, H. S., D. D. Lee, B. Y. Reis, and D. W. Tank (2000). Stability of the memory of eye position in a recurrent network of conductance-based model neurons. *Neuron* 26(1): 259–271.

Soden, M. E. and L. Chen (2010). Fragile X protein FMRP is required for homeostatic plasticity and regulation of synaptic strength by retinoic acid. *J Neurosci* 30(50): 16910–16921.

Stemmler, M. and C. Koch (1999). How voltage-dependent conductances can adapt to maximize the information encoded by neuronal firing rate. *Nat. Neuro.* 2: 512–527.

Triesch, J. (2007). Synergies between intrinsic and synaptic plasticity mechanisms. *Neural Comput* 19(4): 885–909.

Turrigiano, G. G. (2011). Too many cooks? intrinsic and synaptic homeostatic mechanisms in cortical circuit refinement. *Annu. Rev. Neurosci.* 34: 89–103.

van Rossum, M. C. W., M. A. A. Meer, D. Xiao, and M. W. Oram (2008). Adaptive integration in the visual cortex by depressing recurrent cortical circuits. *Neural Comput* 20(7): 1847–1872.

van Welie, I., J. A. van Hooft, and W. J. Wadman (2004). Homeostatic scaling of neuronal excitability by synaptic modulation of somatic hyperpolarization-activated ih channels. *Proc Natl Acad Sci U S A* 101(14): 5123–5128.

Yi, T.-M., Y. Huang, M. I. Simon, and J. Doyle (2000). Robust perfect adaptation in bacterial chemotaxis through integral feedback control. *Proceedings of the National Academy of Sciences* 97(9): 4649–4653.

Zahreddine, Z. and E. Elshehawey (1988). On the stability of a system of differential equations with complex coefficients. *Indian J. Pure Appl. Math* 19: 963–972.

Zenke, F., G. Hennequin, and W. Gerstner (2013). Synaptic plasticity in neural networks needs homeostasis with a fast rate detector. *PLoS computational biology* 9(11): e1003330.

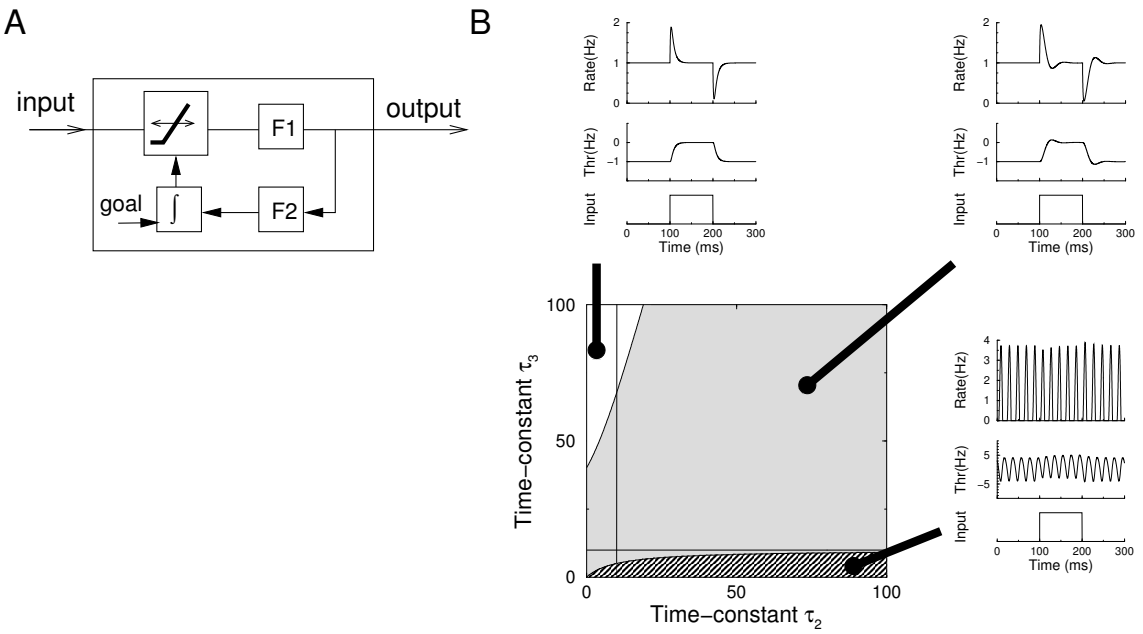

Figure 1: Single neuron homeostasis.
A) Schematic illustration of the homeostatic model. The input current is transformed through an input-output relation and a filter. The input-output curve is shifted by a filtered and integrated copy of the output firing rate, so that the average activity matches a preset goal value. *F1* (time-constant τ_1) denotes a filter describing the filtering between input and output of the neuron; *F2* (time-constant τ_2) is a filter between the output and the homeostatic controller.
B) The response of the model for various settings of the homeostatic time-constants. The value of τ_1 was fixed to 10ms (thin lines), while τ_2 and τ_3 were varied. Center plot: the response of the neuron can either be stable (top left plot; white region), a damped oscillation (top right plot, gray region), or unstable (bottom right plot, striped region). The surrounding plots show the firing rate of the neuron and the threshold setting in response to a step stimulus.

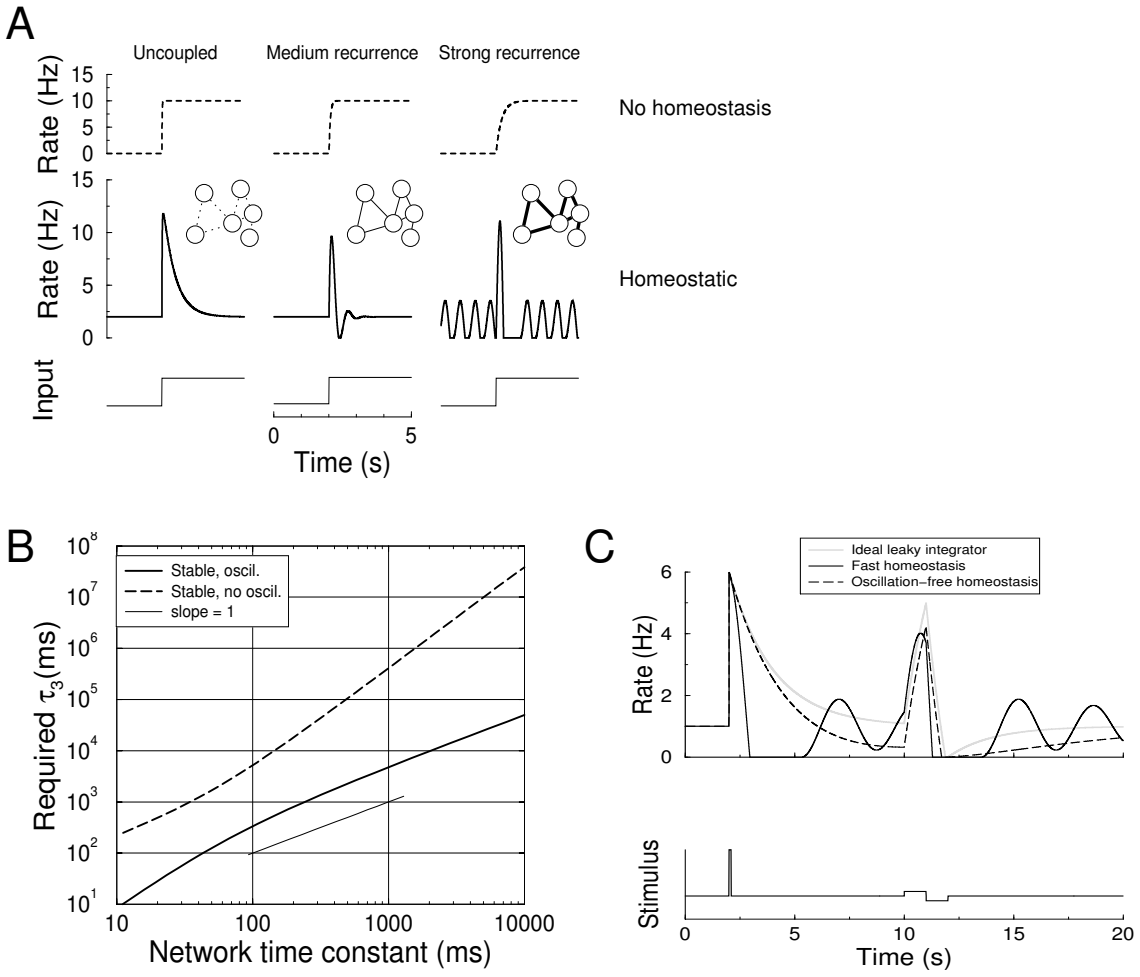

Figure 2: Homeostasis can destabilize activity in otherwise stable networks.
A) Activity in a homeostatic network with varying levels of recurrence, but identical homeostatic parameters ($\tau_1 = 10$ms, $\tau_2 = 50$ms, $\tau_3 = 500$ms). Without homeostasis even the strongly recurrent network is stable (top row). With homeostasis, although the network in stable in the absence of synaptic coupling (left), with increasing recurrence the network shows increasing oscillatory activity (middle, $w_m = 0.8$), and becomes unstable for strong recurrence, leading to unabating oscillations (right, $w_m = 0.95$).
B) The requirements on the homeostatic time-constant as a function of the recurrence of the network, expressed in terms of the network time-constant, which equals $\tau_1/(1 - w_m)$. Shown are the minimal value of τ_3 to ensure stability, potentially with damped oscillations (solid curve) and the minimal value of τ_3 for a stable firing rate without oscillation (dashed curve).
C) The interference of homeostatic control with a neural integrator. The response of an ideal leaky-integrator with 1s time-constant (gray curve) to a pulse at 2s, and a bi-phasic pulse at 10 s. The response of a stable, but oscillatory homeostatic network is very different from the non-homeostatic case (black curve, $\tau_3 = 7$s). Only when the homeostasis is slow enough to be oscillation-free, the response approximates that of the ideal integrator (dashed curve, $\tau_3 = 420$s).

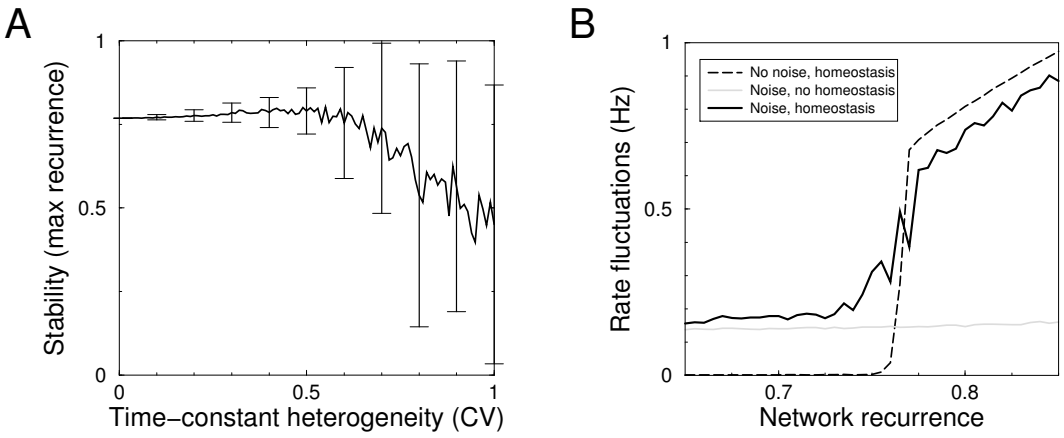

Figure 3: Effects of heterogeneity and noise on homeostatic stability of a network.
A) The stability as a function of heterogeneity in the neurons' homeostatic time-constants. The time-constants τ_1, τ_2, τ_3 for each neuron were drawn from gamma-distributions with means 10, 50 and 100ms, respectively, and a CV given by the x-axis. The curve represents the mean maximal recurrence allowed to ensure a stable system. It decreases with heterogeneity. Error bars represent the standard deviation over 1000 trials. Simulation of 10 neurons, connected with a random, fixed weight matrix.
B) Noise does not ameliorate instability. The fluctuations in the population firing rate, due to both noise and oscillations, are plotted as a function of the network recurrence. Without noise, fluctuations are only present when the recurrence exceeds the critical value (dashed curve). With noise, the fluctuations are already present in the stable regime and increase close to the transition point (solid curve). The homeostasis in the system amplifies noise compared to the non-homeostatic system (grey line). Homeostatic time-constants were 10, 50 and 100ms.

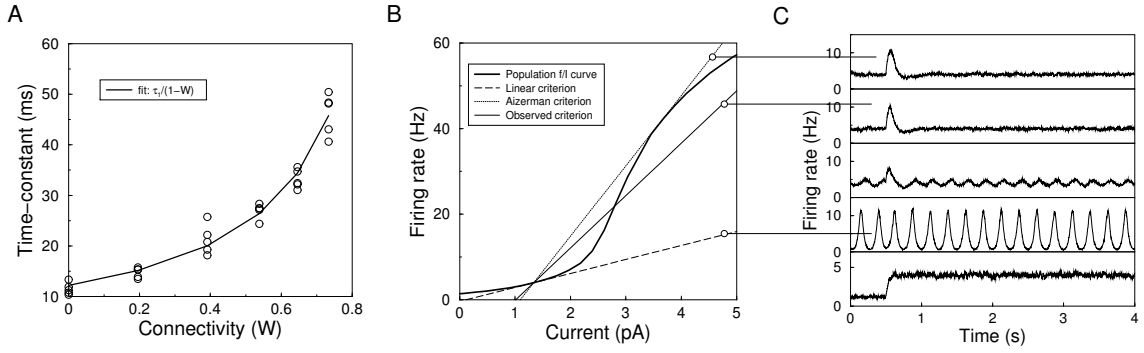

Figure 4: Homeostatic regulation in a network of integrate-and-fire neurons.
A) The effective time-constant of the network as a function of recurrent connection strength. Circles denote simulation results and the curve is the fitted relation $\tau_1/(1-w_m)$.
B) The f-I curve and the stability criterion. The solid curve shows the f-I curve as determined from the simulations with homeostasis turned off. The various lines have a slope proportional to τ_3. According to linear theory stability the minimal τ_3 required is given by the slope at the set point (dashed lined). Stability of a system with a non-linear f-I curve requires the time-constant to be such that the line encompasses the f-I curve (dotted line). In practice stability was achieved for a slightly smaller value of τ_3 (solid line).
C) Example population response to step stimuli for varying values of τ_3 corresponding to the lines in panel B). From top-to bottom: stable according to , $\tau_3 = 322$ms (Aizerman criterion); $\tau_3 = 240$ms (empirically stable); τ_3=200ms (edge of instability); $\tau_3 = 64$ms (linear criterion); Bottom panel: network without homeostasis.

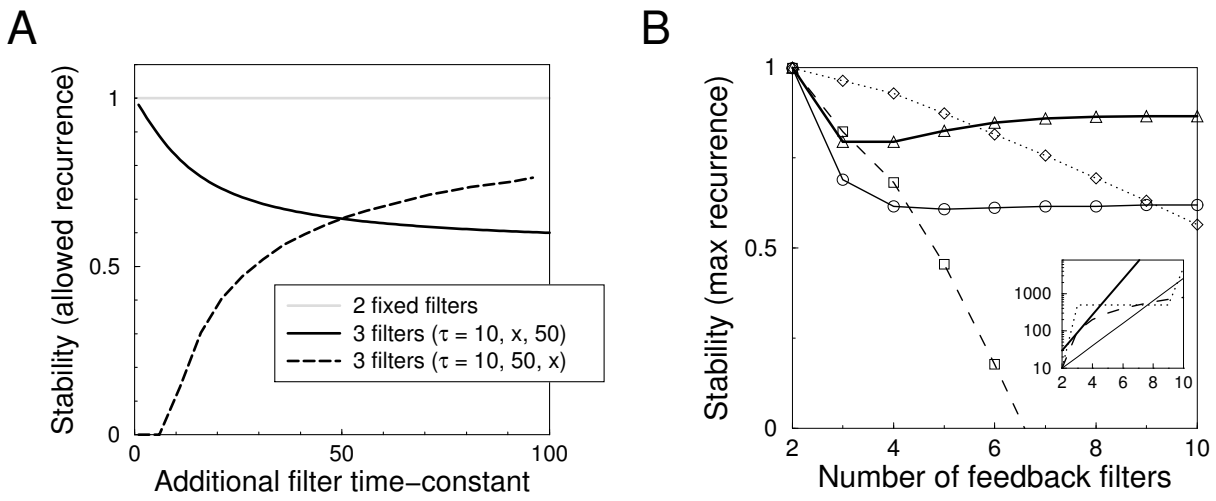

Figure 5: Networks with longer feedback cascade are less stable. A) The effect of adding a third filter to a two filter cascade. The stability is expressed as the maximum recurrence allowed in the network before it becomes unstable (transient oscillations allowed). The system with three filters is always less stable than the two filter system. The time-constants were set $\tau_1 = 10$, $\tau_2 = 50$ in the case of two filters, and $\tau_1 = 10$, $\tau_2 = 50$, $\tau_3 = x$, as well as $\tau_1 = 10$, $\tau_2 = x$, $\tau_3 = 50$ for the three filter case.
B) Stability versus the number of filters for various filter cascades. As a function of filter number, time-constants were set linear $10, 20, 30, 40, \ldots$ (dashed), constant with slow final integrator $10, 500, 500, \ldots, 500, 5000$ (dot-dashed), or exponential $10, 20, 40, \ldots$ (solid) and $10, 30, 90, \ldots$ms (thick solid). The inset show the time-constants for a cascade with 10 filters for the various cases. Except for the last case, stability decreases with the number of filters.